Chapter 23. Radial and planar axes, mapping distortions and cytoplasmic flux.

During interphase, AJs are distributed around the Par-3/Par1 boundary, in line with the epithelial surface contours. However, the lateral boundaries of asynchronously dividing epithelial cells tend to be irregular and fluid, with random mitotic spindle orientation in the epithelial plane. During terminal PCP signalling, Ap surface contraction may generate uniformly packed hexagonal cells in the wing blade, with AJs tending to localise to cellular vertices. While regular hexagonal cells may tile the wing blade with only minor defects, wrapping an epithelial sheet around the curved a surface of the embryo must distort cellular interfaces, particularly as the cells are large with respect to the surface curvature of the egg. Such topological constraints play out sequentially during the mid-blastoderm transition and the subsequent convergent-extension movements of gastrulation.

In *Drosophila*, fertilisation takes place through dorsal anterior micropyles, which triggers the meiosis of both the egg and sperm pro-nuclei. The four haploid pro-nuclei fuse to form two diploid nuclei at the egg centre; which divide with random spindle orientations [1]. Thus, in contrast to the mouse or worm model systems, the initial fertilisation and nuclear divisions of *Drosophila* cannot set the embryonic axes. In this context, the syncytial nuclei migrate outwards from the egg centre during the 7^{th}-13^{th} divisions. The first nuclei arrive at the posterior pole in cycle 9 and bud-off to form an asynchronous pole-cell population. The remaining nuclei populate the egg cortex during cycle 10. In principle, the position of each cortical nucleus could be defined with respect to a radial co-ordinate from the egg centre and an angular displacement from the ventral midline. Notably, the polyploid yolk nuclei and yolk granules oscillate centripetally during the syncytial blastoderm divisions. These radial movements are in synchrony with polar mitotic waves and polar/equatorial displacements of cortical periplasm [2 3]. These oscillations are consistent with reversals in microtubule motor activities along radially aligned microtubules, together with actomyosin driven movements of the cortical periplasm. Such movements might cause turbulent mixing of maternal factors, however, the sulphated anchor inscribed on the ventral vitelline membrane would remain undisturbed (see above, Chapter **22**) as should any nuclear-bound morphogenetic factors. At the egg cortex, the arrival of each nucleus induces the formation of a superficial bud containing both actin and microtubule filaments. Polar/equatorial waves may be transmitted across the rims of these shallow cups, but their major function is to act as spindle anchor points. This mechanism aligns mitotic spindles with the blastoderm surface [2 4]. Thus, the boundaries of the somatic buds separate adjacent nuclei, although the distribution of mitotic spindles is somewhat uneven with occasional gaps. Neighbouring nuclei are closely packed, but their mitotic spindles are misaligned with respect to the embryonic axes, see Fig. 5 in [5].

Cytoskeletal remodelling of the syncytial blastoderm may be triggered by transcription of *WntD*, which is initiated in a few nuclei near the embryonic poles [6]. By the mid-blastoderm transition, the polar caps have been cleared of both yolk granules and the translated WntD protein. Meanwhile, radial membrane downgrowth from the rims of the cortical blebs separates syncytial nuclei within individual cells, and Par-1 is localised to the Ba cellular compartment. The ventral furrow forms along about 70% of the embryonic mid-line, stopping short of the poles [2]. The ends of the furrow are delimited by A and P midgut rings, which may set the radial axis of the gut epithelium (see below, Chapter **29**). Meanwhile, the pole cells pass through the P mid-gut ring, before migrating across the Ba surface of the abdominal epithelium to populate the genital ridge. The Ap surface of ventral mid-line cells contracts during furrow formation, with contractile MyoII pulses [7]. During these cell shape changes, actin filaments extend across several cell diameters, anchored through the extracellular matrix. Arm (β-Catenin) functions

as a transcriptional activator of Wg/Wnt signalling pathways, as well as forming a structural component of AJs [8 9 10]. Meanwhile, WntD binds the Fz4 receptor to block the extracellular domain of Tl [11]. Thus, Arm is a core component of mechanically coupled signal transduction across lateral cell interfaces.

Cell shape changes along the ventral furrow and during the convergent-extension movements of gastrulation are driven by contractile pulses of MyoII activity in the Ap cortical periplasm [7]. The MyoII motors may act as simple, double-headed cargo transporters or assemble into braided, bipolar mini-filaments, with multiple motor heads, see below **30**. MyoII mini-filaments can template the assembly of ordered F-actin arrays in syncytial muscles. By contrast, in the periplasm of epithelial cells most of the F-actin filaments are labile, with only the outer layer being anchored directly to the extracellular matrix. In consequence, MyoII mini-filaments may nucleate and drive F-actin filaments apart. During the mid-blastoderm transition, mechanical tension transmitted through lateral cell interfaces generates a coupled cytoplasmic flux of MyoII-GFP around the embryonic cortex (Fig. 29).

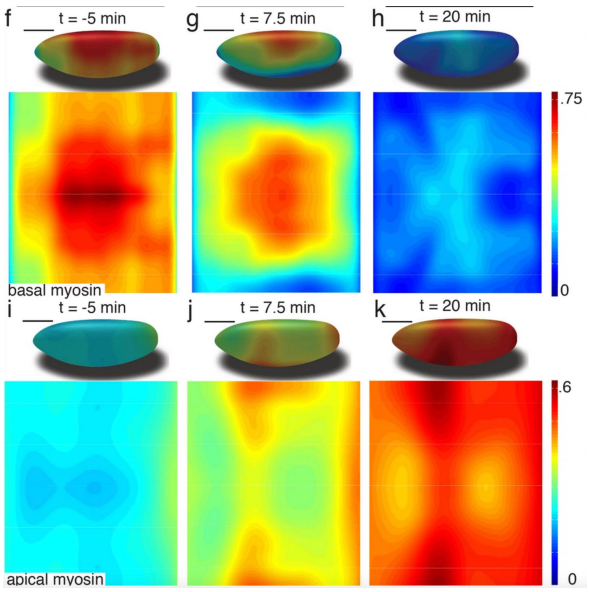

Fig. 29. Embryonic MyoII flux. Immediately following membrane in-growth during blastoderm cellularisation, cortical actomyosin filaments become coupled through lateral cell interfaces. A saddle point develops along the dorsal equatorial midline; with basal localisation of MyoII-GFP, and minimal flux on the Ap cortical surface. From Streichan et al. 2018.

Strikingly, the cortex is divided into four quadrants, with alternating clockwise and anticlockwise vortices [12] (Fig. 30). The Ap MyoII-GFP shows increased form optical birefringence, consistent with the assembly of braided mini-filaments, with multiple MyoII motor domains. Meanwhile, the internal cytoplasmic flux may track inactive MyoII-GFP punctae as microtubule cargos, driven by Dynein motors. In addition, Kinesin cartwheel assemblies may drive apart telescoping microtubule filaments, and contribute to the cytoplasmic flux, with translocated MyoII-GFP (see below Chapter **30**). As cellularisation is completed a saddle point develops along the dorsal equatorial midline, with basal localisation of MyoII-GFP and minimal flux in the surface plane [12] (Fig. 29, 30). A ventral equatorial saddle becomes visible slightly later.

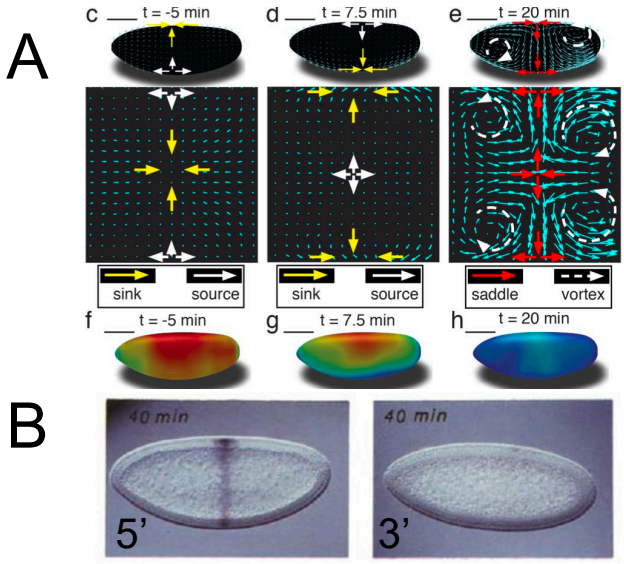

Fig. 30. A contractile actomyosin-driven flux separates the embryonic cortex into four quadrants, with alternating clockwise and anticlockwise vortices and cruciform saddle points **A**. From, Streichan et al., 2018. **B.** The equatorial midline is also manifest by the initiation of transcription of *Ubx*, 40 mins after start of cycle 13 (before complete cellularisation). However, full-length *Ubx* transcripts are not formed until germ-band extension, late in cycle 14. Left panel 5' Ubx *in situ*. Right panel 3' *Ubx in situ*, from Shermoen and O'Farrell, 1991.

Taken together, these results are consistent with cytoplasmic remodelling being dependent on the Frank elastic moduli of fibrillar components, with non-Newtonian fluid drag contributing to fibril alignment. By implication, neither the polar/equatorial waves, nor the chiral vortices across the cellular blastoderm, are initiated from discrete foci. Instead, cytoplasmic flux is constrained by the internal topography of the oocyte; with checkpoint release coupled to global fluctuations in cyclin activities. In this sense, the embryonic axial system may be generated as a harmonic standing wave, with virtual origins near the A and P poles. After the A and P mitotic waves arrest at the embryonic equator, a drop in Cyclin A and B levels may allow formation of novel polar foci, from which the subsequent polar waves are released. During the 13th cycle, transcription of *Ubx* marks the equatorial mid-line, although full-length transcripts are not completed before gastrulation [13] (Fig. 30). During gastrulation, the MyoII-GFP flux tracks the pair-rule stripes of Eve [12]. Germ-band extension is driven predominantly by actomyosin contractions around the circular (D/V, L/R) embryonic axis, although preferential microtubule growth along the oblate (A/P) axis may also contribute.

As cells elongate, MyoII is localised to A/P interfaces (regulated by Rho kinase), while and Par-3 (Baz) is localised along their D/V (L/R) boundaries [14]. Meanwhile, the alignment of F-actin microfibrils is regulated via Rho-GEF2, with E-Cad and the Abl kinase localised to D/V (L/R) cellular interfaces [15]. In consequence, co-ordinated waves of contraction and extension push the terminal abdominal segments around the P pole. During these movements, lateral cell interfaces are aligned with the ventral midline, forming elongated, oblong cells. Towards the end of germ-band extension, mitotic spindle planes become aligned with the parasegmental (Wg/En) boundaries, (the Foe, serially repeated

domain $\delta_{14}25$). At this stage, *wg* mutant embryos can be rescued by Ap (radially) localised *wg* mRNA [16 17]. Taken together, these results show that Ap translation of *wg* may precede the trafficking of Wg-tagged MVBs along the long (A/P) embryonic axis [8 18]. As in the oocyte, microtubule cargos may be attached to either plus-end, or minus-end, directed motors, with active transport towards either embryonic pole. However, while a global axial system follows the embryonic surface topography, local cellular axes may be re-set with respect to segmental boundaries and parasegmental AMSs. During gastrulation, infolding boundary cells may constrain convergent-extension movements, as segmental folds develop along the A/P embryonic axis. Thus, AJ localisation around the Ap/Ba (Par1/Par3) cortical interface may define planar spindle axes during prophase and displace the Ap/Ba axis of adjacent cells during cytokinesis. In consequence, polarised cargo transport and cytoplasmic remodelling drive the mid-blastoderm transition and gastrulation, with asymmetric partitioning of morphogenetic factors.

Summary:

The embryonic axial system in *Drosophila* is progressively refined following the radial migration of syncytial nuclei from the centre of the egg. Cortical mitotic waves are initiated near the embryonic poles to converge at the equatorial mid-line, with radial oscillations of yolk nuclei, and A/P displacement of cortical periplasm. Syncytial mitotic spindles align around the embryonic cortex, with random orientations in the surface plane. Radial membrane downgrowth from cortical surface separates individual nuclei during cellularisation. At this stage, transmembrane-coupled cytoplasmic flux divides the embryonic cortex into four quadrants (AD, AV, PD, PV), with subsequent sub-divisions along the A/P embryonic axis. Following cellularisation, the alignment of coupled cytoplasmic interfaces directs polarised cargo transmission, morphogen flux and asymmetric partitioning. Mitotic spindle axes are aligned to either side of the ventral (L/R) midline, and parasegmental AMSs along the A/P axis. Motor-protein complexes are assembled, disassembled, and trafficked as cargo components; with labile cytoskeletal filaments, transmembrane anchors, against non-Newtonian fluid drag. In consequence, mechanical anchoring may drive co-ordinated cell shape changes across morphogenetic twin-fields and align mitotic spindles orientations at their boundaries.

References:

1. Campos-Ortega, J. A. & Hartenstein, V. *The Embryonic Development of Drosophila Melanogaster*. (Spriger-Verlag, Berlin, 1985).
2. Foe, V. E. & Alberts, B. M. Studies of nuclear and cytoplasmic behaviour during the five mitotic cycles that precede gastrulation in Drosophila embryogenesis. *J. Cell Sci.* **61**, 31–70 (1983).
3. Miller, K. G., Field, C. M. & Alberts, B. M. Actin-binding proteins from Drosophila embryos: a complex network of interacting proteins detected by F-actin affinity chromatography. *J. Cell Biol.* **109**, 2963–2975 (1989).
4. Mermall, V. & Miller, K. G. The 95F unconventional myosin is required for proper organization of the Drosophila syncytial blastoderm. *J. Cell Biol.* **129**, 1575 (1995).
5. Foe, V. E. Mitotic domains reveal early commitment of cells in Drosophila embryos. *Development* **107**, 1–22 (1989).

6. Ganguly, A., Jiang, J. & Ip, Y. T. Drosophila WntD is a target and an inhibitor of the Dorsal/Twist/Snail network in the gastrulating embryo. *Development* **132**, 3419–3429 (2005).
7. Vasquez, C. G., Tworoger, M. & Martin, A. C. Dynamic myosin phosphorylation regulates contractile pulses and tissue integrity during epithelial morphogenesis. *J. Cell Biol.* **206**, 435–450 (2014).
8. Bejsovec, A. & Wieschaus, E. Signaling activities of the Drosophila wingless gene are separately mutable and appear to be transduced at the cell surface. *Genetics* **139**, 309–320 (1995).
9. Jones, W. M. & Bejsovec, A. RacGap50C negatively regulates wingless pathway activity during Drosophila embryonic development. *Genetics* **169**, 2075–2086 (2005).
10. Bejsovec, A. Wingless/Wnt signaling in Drosophila: the pattern and the pathway. *Mol. Reprod. Dev.* **80**, 882–894 (2013).
11. Rahimi, N. *et al.* A WntD-dependent integral feedback loop attenuates variability in Drosophila Toll signaling. *Dev. Cell* **36**, 401–414 (2016).
12. Streichan, S. J., Lefebvre, M. F., Noll, N., Wieschaus, E. F. & Shraiman, B. I. Global morphogenetic flow is accurately predicted by the spatial distribution of myosin motors. *eLife* **7**, (2018).
13. Shermoen, A. W. & O'Farrell, P. H. Progression of the cell cycle through mitosis leads to abortion of nascent transcripts. *Cell* **67**, 303–310 (1991).
14. Simões, S. M. *et al.* Rho-Kinase directs Bazooka/Par-3 planar polarity during Drosophila axis elongation. *Dev. Cell* **19**, 377–388 (2010).
15. Barrett, K., Leptin, M. & Settleman, J. The Rho GTPase and a putative RhoGEF mediate a signaling pathway for the cell shape changes in Drosophila gastrulation. *Cell* **91**, 905–915 (1997).
16. van den Heuvel, M., Nusse, R., Johnston, P. & Lawrence, P. A. Distribution of the wingless gene product in drosophila embryos: A protein involved in cell-cell communication. *Cell* **59**, 739–749 (1989).
17. Simmonds, A. J., dosSantos, G., Livne-Bar, I. & Krause, H. M. Apical localization of wingless transcripts is required for Wingless signaling. *Cell* **105**, 197–207 (2001).
18. Strigini, M. & Cohen, S. M. Wingless gradient formation in the Drosophila wing. *Curr. Biol.* **10**, 293–300 (2000).